

"Enhancing Image Quality Through Denoising Using the Sliced Ridgelet Transform Technique"

Dr.Aravind Prasad

1. Ph. D. Research Scholar, Dept of ECE, Mewar University, Chittorgarh, Rajashtan, India.
2. Professor, Department of ECE, Mewar University, CET, Chittorgarh, Rajashtan, India.

ABSTRACT: Image quality is crucial for various applications in image and video processing. Often, the quality of captured images falls short of expectations due to the presence of noise. Noise adversely affects image processing and related decision-making applications, leading to inaccurate and erroneous results. Therefore, image denoising is a fundamental requirement for effective image and video processing. While several previous studies have introduced various approaches to this problem, challenges related to accuracy, quality, and reliability persist.

This thesis focuses on developing a precise and scalable image denoising method to achieve high-quality results that surpass existing technologies in image and video processing. To address the aforementioned challenges, we propose an integrated and comprehensive solution using the Sliced Ridgelet Transform for image denoising. This research introduces the Sliced Ridgelet Transform, a technique that offers improved scalability, accuracy, and reliability in image processing. The method involves computing ridgelets in a localized manner, which is computationally less intensive compared to curvelets while providing similar denoising performance. The Sliced Ridgelet Transform divides the ridge function into multiple slices of constant length, utilizing single-dimensional wavelet transforms to calculate the angle values for each slice. Ridgelet coefficients are then used for base threshold calculations to implement accurate denoising.

The proposed method for image denoising involves two main operations: a redundant directional wavelet transform based on the Radon transform and the design of thresholds for the ridgelet coefficients. This research compares the accuracy and scalability of the Sliced Ridgelet Transform with other popular methods such as wavelets, curvelets, and other relevant technologies. Experimental results demonstrate that the Sliced Ridgelet approach outperforms these other techniques in terms of performance.

KEYWORDS: Ridgelet Transform, Image Denoising, Curvelets, Ridgelet coefficient, Ridge function.

I. INTRODUCTION

In today's digital age, the use of images has surged across various domains, including fashion, art, design, animation, advertising, and fingerprint identification. Image processing is a fundamental technology for numerous real-time applications such as image search engines, image clustering, image segmentation, and entropy detection. One of the key attributes of an image is its clarity, which refers to the resolution and sharpness of its pixels. High image clarity is crucial for achieving accurate and reliable results in image processing applications. Enhanced clarity significantly improves result accuracy and reliability.

Image blurriness, often referred to as image noise, is a common issue in image processing that needs to be addressed before further analysis. To effectively compare, segment, and cluster images, it is essential to remove noise, a process known as image denoising. This step is critical for reducing the challenges and bottlenecks in image processing, ensuring clearer and more precise outcomes.

The recent proposed procedures by various authors has been introduced image de-noising based on transforms such as wavelets, curvelets, exploit redundancy and threshold to remove the noise without blurring the edges. Although many previous approaches have been introduced in this area so far, none of them are resolved the image noising issue up to the expected level of image processing. Although wavelet transform is the better existing technology than others it is also suffering from some transformation problems like Shift sensitivity, Poor Directionality and Absence of Phase information. In recent ridgelet transforms proven that, they are better than wavelet transforms [1] to implement the denoising procedure for images in image processing applications.

In this research, we introduced “Sliced Ridgelet Transform for Image De-noising” to mitigate the burden of image denoising process and to improvise the image display resolution depth (image clarity) to extract the best results while working with image processing applications. This scheme also addresses the main issues and disadvantages of wavelet transform like Shift sensitivity, Poor Directionality and Absence of Phase information while doing the image denoising process. The important characteristic of the de-noising technique introduced in this project is that it can reduce considerably the noise without destroying the edges of the objects in the image. Experimental results with MATLAB software is proving our thesis scalability, accuracy and reliability while comparing with other schemas like wavelet transform and curvelet transform. These results were stated that, usage of sliced ridgelet transform model is having the better performance than other transform schemas.

II. RELATED WORK

2.1 SLICED RIDGELET TRANSFORM:

In this section, we present our proposed Sliced Ridgelet Transform technology and outline the contributions of this thesis. We begin by introducing the Sliced Ridgelet Transform, including its terminology and foundational concepts. Next, we detail the objectives of our research, exploring our innovative approach to the Sliced Ridgelet Transform and its associated technologies in a structured and interconnected manner. The first phase of this section covers the basic Ridgelet Transform and its mathematical implementation. The second phase focuses on image slicing and the implementation of the Sliced Ridgelet Transform. The third phase addresses issues related to shift sensitivity in wavelets, discusses threshold values, and examines the Sliced Ridgelet Transform algorithm. Image denoising, which is critical for effective image processing and its applications, is the core focus of our study. While popular image denoising technologies include wavelet transforms, curvelet transforms, and Ridgelet transforms, the Ridgelet Transform was introduced to address the challenges of redundancy and performance limitations in image processing. These issues have historically led to inaccurate results and inconsistencies.

Recently, the Ridgelet Transform has emerged as a viable alternative to wavelet transforms, overcoming some of their limitations. The 2D wavelet transform often results in numerous large coefficients across various scales, which complicates the denoising of noisy images. The Sliced Ridgelet Transform aims to mitigate these difficulties by providing a more efficient and effective approach to image denoising.

This is become a big problem in processing of images with an efficient legacy wavelet mechanism. Ridgelet transform was successfully applied on digital image processing with different orientations and locations. Unlike wavelet transforms [6 and 7], the ridgelet transform processes data by first computing integrals over different orientations and locations. A ridgelet is constant along the lines $x_1 \cos \beta + x_2 \sin \beta = \text{constant}$. In the direction orthogonal to these ridges it is a wavelet. Ridgelets have been successfully applied in image de-noising recently.

Ridgelets is a novel feature in image processing, which applied in the research area of image de-noising. For each $a > 0$, each $b \in \mathbb{R}$ and each $\Theta \in [0, 2\pi)$, the bipartite ridgelet (\cdot, a, b) : $\mathbb{R}^2 \rightarrow \mathbb{R}$ is defined as

$$\lambda(a, b, \theta) = a^{(-1/2)} \lambda((x_1 \cos \theta + x_2 \sin \theta - b)/a),$$

where λ is a predefined wavelet method. Ridgelet value is static with the lines

$$\lambda(x1 \cos x) + \lambda(x2 \sin y) = \text{static constant.}$$

Diagonal to these ridges it is a well formed wavelet. Given an invariant bipartite image $f(x1, x2)$, and we can write its ridgelet (for each $(p > 0)$ and $(q \in R)$) significant formula as:

$$R(p, q, \theta) = p, q, \theta, f(\lambda(x1, x2) d(x1) d(x2)).$$

The given below figure 1 shows the basic ridgelet function with its sliced transforms.

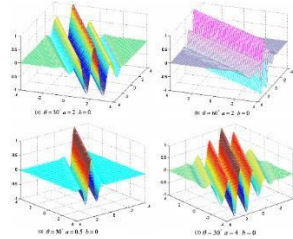


Fig 1 Basic Sliced ridgelets formation with various angular variable θ values

The above diagram specifies the various constant θ values and their respective ridgelets curved area of an image. By varying the values of a and θ we just shown the image representations. As per the requirement these ridgelets might be scaled, shifted and rotated also.

Sliced ridgelet transform is a multi-dimensional and precise wavelet transform with slices. In this approach the θ is a random static constant and the a value will be change frequently. Ridgelets are quite varied from wavelets in the view of ridgelets parade very high directional sensitivity and are highly anisotropic. This high anisotropic value is caused to get the best results while implementing the image de-noising techniques. An exceeded ridgelet transform can be performed in the Fourier domain. Initially for the given image the 2D FFT [8 and 9] is computed. Interpolation process will continue with along a number of straight lines equal to the selected number of projections. Each line passes through the center of the 2D frequency space, with a slope equal to the projection angle, and the number of interpolation points equal to the number of rays per projection. After the 1D inverse FFT along each interpolated ray, we perform a 1D wavelet transform. For Example, for an image with N bit per pixel, and slicing the image with a distinct constant pixel value will effects the results of image processing is called data compression. If we consider there is an image with 8-bits per pixel can represented to bit plans as shown below. In this case zero is the least significant bit (LSB) and 7 is the most significant bit (MSB):

- I. 0 which results in a binary image, i.e, odd and even pixels
- II. 1 which displays all pixels with bit 1 set: 0000.0010
- III. 2 which displays all pixels with bit 2 set: 0000.0100
- IV. 3 which displays all pixels with bit 3 set: 0000.1000
- V. 4 which displays all pixels with bit 4 set: 0001.0000
- VI. 5 which displays all pixels with bit 5 set: 0010.0000
- VII. 6 which displays all pixels with bit 6 set: 0100.0000
- VIII. 7 which displays all pixels with bit 7 set: 1000.0000

Here in the given below figure 3 we can observe some examples of sliced images at various bit planes.

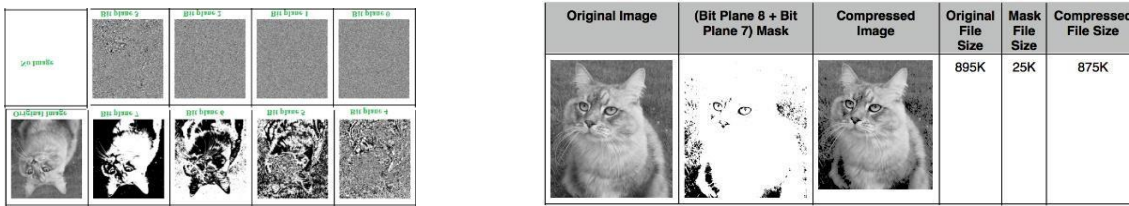


Fig 3. An 8-bit image and different bit-planes after slicing, Fig 4 An 8-bit image compression with mask 7-bit plane

The above image 3 represents the pgm image with 8 different bit planes, which starts from 0 and continues upto 7 (total 8 images). In the next figure 4 shows that a compressed image with 7 bit plane mask and the size comparison also can be seen. From that comparison we understood that, the compressed image size is less than the original image, even after compressing with the 7 bit plane mask.

Advantages of Image Slicing:

- ★ Highlighting the contribution made by a specific bit and For pgm images, each pixel is represented by 8 bits.
- ★ Each bit-plane is a binary image and Less the size even after compression with bit plane
- ★ Processing done at each bit (pixel) level and Result Accuracy, scalability and Reliability

2.2 RADON TRANSFORM

As specified above our sliced ridgelet transform is using the Radon transform technique for 1-D and 2-D for fourier and wavelet transformation sake. Various image layers and their packed pixel content will be calculated by the approximate Radon transform formula is:

Coefficients can be calculated as:

$$w_{j+1}(\vartheta, \varphi) = c_j(\vartheta, \varphi) - c_{j+1}(\vartheta, \varphi)$$

Hence the Radon transform function is:

$$\hat{\psi}_{\frac{l_c}{2^j}}(l, m) = \hat{\phi}_{\frac{l_c}{2^{j-1}}}(l, m) - \hat{\phi}_{\frac{l_c}{2^j}}(l, m)$$

In the recursive manner:

$$\hat{w}_{j+1} = \hat{h}_j \hat{G}_j$$

$$\text{where } \hat{G}_j(l, m) = \begin{cases} \frac{\hat{\psi}_{\frac{l_c}{2^{j+1}}}(l, m)}{\hat{\phi}_{\frac{l_c}{2^j}}(l, m)} & \text{if } l < \frac{l_c}{2^{j+1}} \text{ and } m = 0 \\ 1 & \text{if } l \geq \frac{l_c}{2^{j+1}} \text{ and } m = 0 \\ 0 & \text{otherwise} \end{cases}$$

$$\text{Here, } \hat{G}_j(l, m) = 1 - \hat{H}_j(l, m)$$

In the above given formula set, most of the Radon transforms not have been the invertible transforms for digital images. Meanwhile the Radon transform theory introduced another new interesting topic of transform with by inheriting periodization.

After this invention, Radon Transform has been updated to Slice Support Radon Transform (SSRT), to provide the better support for sliced ridgelet transform. This Slice Support Radon Transform is defined as summations of image pixels over a certain set of “lines.” Those lines are defined in a finite geometry in a similar way as the lines for the continuous Radon transform in the Euclidean geometry [17].

The SSRT for sliced ridgelets was customized as shown below:

$$r_k[l] = FRAT_f(k, l) = \frac{1}{\sqrt{p}} \sum_{(i,j) \in L_{k,l}} f[i, j].$$

$$L_{k,l} = \{(i, j): j = ki + l \pmod{p}, i \in \mathbb{Z}_p\}, \quad 0 \leq k < p,$$

$$L_{p,l} = \{(l, j): j \in \mathbb{Z}_p\}.$$

Here, $L_{k,l}$ denotes the set of points that make up a line on the \mathbb{Z}_p^2 lattice, or, more precisely and i, j are the temp values, p is a prime number and k is the number of vertical lines. The measurable sliced ridgelet co-efficient of an image object f are given by analysis of the Radon transform via:

$$R_f(a, b, \theta) = \int Rf(\theta, t) \psi\left(\frac{t-b}{a}\right) dt$$

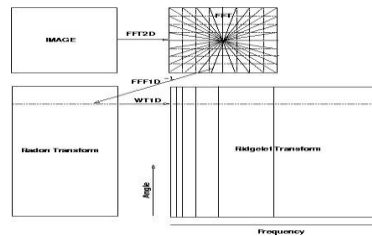


Figure 5 Radon Transform for Sliced Ridgelets

2.3 SLICED RIDGELET TRANSFORM IMPLEMENTATION

The sliced ridgelet transform implementation for digital images at lines, we use this approach as follows

$$L_{[p,q]}^\omega = \left\{ (x_1, x_2) \in \mathbb{Z}^2 \mid |qx_1 - px_2| \leq \frac{\omega}{2} \right\} \text{ with } [p, q] \in \mathbb{Z}^2 \text{ the direction of}$$

the Radon projection and w , a function of (p, q) , the arithmetical thickness. Reveilles introduced the discrete analytical lines defined as $0 \leq qx - py + r < w$. In this thesis, since we need central symmetry, we chose a variant of the closed discrete analytical lines, defined as $0 \leq qx - py \leq w$.

It is easy to see that the closed discrete analytical lines $L_w [p, q]$ have a central symmetry regardless of the value of w . Moreover, the discrete analytical line can easily be extended to higher dimensions as discrete analytical hyper planes. The arithmetical thickness w is an important parameter that controls, among other things, the connectivity of the discrete lines: let's consider the closed discrete analytical line $L_w [p, q]$ and its Euclidean counterpart $L[p, q] : qx_1 - px_2 = 0$, then:

- ★ For $w < \max(|p|, |q|)$, $L_w [p, q]$ is not connected; ★ For $w = \max(|p|, |q|)$, $L_w [p, q]$ is 8-connected.

This is called the closed naive line. It is directly related to the distance d_1 since:

$$L_{[p,q]}^{\max(|p|, |q|)} = \left\{ M \in \mathbb{Z}^2 \mid d_1(M, \mathcal{L}_{[p,q]}) \leq \frac{1}{2} \right\}$$

$$\text{with } d_1(A, B) = |x_1^A - x_1^B| + |x_2^A - x_2^B|$$

- ★ For $w < \max(|p|, |q|)$, $L_w [p, q]$ is 8 connected;
- ★ For $w = \max \text{sqrt}(|p|, |q|)$, $L_w [p, q]$ is 8-connected.

$$L_{[p,q]}^{\sqrt{p^2+q^2}} = \left\{ M \in \mathbb{Z}^2 \mid d_2(M, \mathcal{L}_{[p,q]}) \leq \frac{1}{2} \right\}$$

$$\text{with } d_2(A, B) = \sqrt{(x_1^A - x_1^B)^2 + (x_2^A - x_2^B)^2}$$

These results are direct consequence of a well-known result in discrete analytical geometry and more recent studies on distances. The fact that these lines can be defined with help of distances makes a direct link with mathematical

morphology. We use the Fourier domain for the computation of Fast Fourier Radon transform: Fourier coefficients of s are extracted along the discrete analytical line $L^w[p, q]$.

$$P_{[p,q]}^\omega s = \bigcup_{k \in \mathbb{Z}^+} \hat{s}(f_1^k, f_2^k) \text{ such that } |qf_1^k - pf_2^k| \leq \frac{\omega}{2}$$

and we take the 1-D

inverse FFT of $P_w[p, q]$ s on each value of the direction $[p, q]$. Formally, our discrete analytical Radon transform is defined by:

$$R^w s([p, q], b) = \sum_{k=0}^{K-1} P_{[p,q]}^\omega s(k) \cdot e^{2\pi j \frac{k}{K} b} \text{ with } K \text{ length of } L_{[p,q]}^\omega$$

We must define the set of discrete directions $[p, q]$ in order to provide a complete representation. The set of line segments must cover the entire square lattice in the Fourier domain. For this, we define the directions $[p, q]$ according to pairs of symmetric points from the boundary of the 2-D discrete Fourier spectra as shown in figure 6.

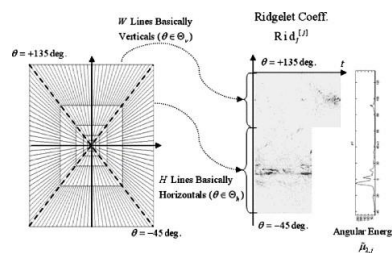


Figure 6 Sliced Ridgelet Transformation for line Singularities

PROPOSED ALGORITHM - SLICED RIDGELET DE_NOISING ALGORITHM

Begin

Input: digital image corpus with noise Output:

de-noised digital image corpus Process:

Step1: Start image partition as horizontal and vertical $R \times R$ blocks

Step2: Arrange the vertical overlapping for adjacent block as $R/2 \times R$

Step3: Arrange the horizontal overlapping for adjacent block as $R \times R/2$ \ Step4:

for Each (block: $R \times R$) {

- *Apply image slicing*
- *Get smaller number of coefficients*
- *Apply FastFourierTransform (FFT)*
- *Apply Radon Transform*
- *Set Threshold value*
- *Run sliced ridgelet transform*

}

Step5: Collect the same location pixel values at donoising image

Step6: Generate process phase wise result report and display them

End

We call this algorithm as Sliced RidgeletShrink, while the algorithm using the ordinary RidgeletShrink. The computational complexity of Sliced RidgeletShrink is similar to that of RidgeletShrink by using the scalar wavelets. The only difference is that we replaced the 1D ridgelet transform with the 1D dual-tree sliced ridgelet transform. The amount of computation for the 1D dual-tree sliced ridgelet is twice that of the 1D scalar wavelet transform. However, other steps

of the algorithm keep the same amount of computation. Our experimental results show that sliced RidgeletShrink outperforms VisuShrink, RidgeletShrink, and wiener2filter for all testing cases. Under some case, we obtain 1.30 dB improvements in PSNR over RidgeletShrink. The improvement over VisuShrink is even bigger for denoising all images. This indicates that Sliced RidgeletShrink is an excellent choice for de-noising natural noisy images.

This whole process is explained in detail of the experiments section

III. SIMULATION RESULTS

The In this section we discuss about the image de-noising experiments in detail with our proposed sliced ridgelet transform methodology. In these experiments, we simulate noisy images by corrupting the 512 x 512 textured grass images with 10 different realizations of WGN with standard deviation 25. The noisy images are then de-noised with various existing methodologies and our sliced ridgelet transform environment. we implement VisuShrink, RidgeletShrink, SlicedRidgeletShrink and wiener2. VisuShrink is the universal soft-threshold denoising technique. The wiener2 function is available in the MATLAB Image Processing Toolbox, and we use a 5x5 neighborhood of each pixel in the image for it. The wiener2 function applies a Wiener filter (a type of linear filter) to an image adaptively, tailoring itself to the local image variance. The experimental results in PSNR are shown is for de-noising Lena image for different image partition block sizes by using ComRidgeletShrink. It can be seen that the partition block size of 32x32 or 64x64 is our best choice as shown in figure 7. In MRI Scan experiment, for different noise levels and a fixed partition block size of 32x32 pixels. The first column in these tables is the PSNR of the original noisy images, while other columns are the PSNR of the de-noised images by using different denoising methods along with our proposed sliced ridgelet transform and the result is as shown in below figure 7.

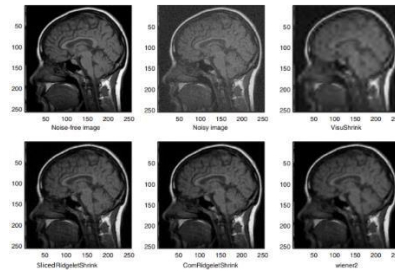
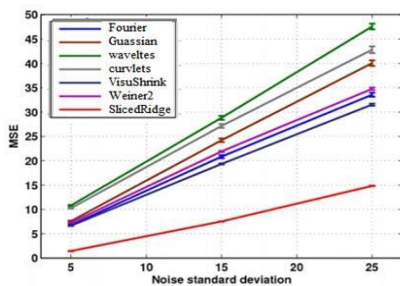


Figure 7 MRI Scan Experiment with various image de-noising methodologies,



Noisy image	VisuShrink	RidgeletShrink	SlicedRidgeletShrink	wiener2
34.12	29.49	36.67	37.19	30.96
28.10	26.31	32.51	33.13	30.09
24.58	24.77	30.23	30.79	29.04
22.08	23.85	28.63	29.21	28.01
20.14	23.24	27.39	28.00	27.07
18.56	22.83	26.39	27.03	26.22

From Tables 1 we can see that SlicedRidgeletShrink outperforms VisuShrink, the ordinary RidgeletShrink, and wiener2 for all cases. VisuShrink does not have any denoising power when the noise level is low. Under such a condition, VisuShrink produces even worse results than the original noisy images. However, SlicedRidgeletShrink performs very well in this case. For some case, SlicedRidgeletShrink gives us about 1.30 dB improvements over the ordinary RidgeletShrink. From figure we compare the de-noising performance for various methods for the synthetically generated stripes image containing multiple exact replicas of each line singularity.

Figure 8 MRI Scan Image donoising comparison, Table 1 MRIScan Comparison with various donoising techniques For strong noise, the non-local methods, namely VisuShrink, Weiner2 and Guassian, Sliced Rigelet clearly outperform the local approaches. High levels of redundancy as well as low patch complexity result in our bounds predicting a very small lower bound even for quite strong noise levels. Comparing performances of the state-of-the-art methods to the bounds allows us to gauge the room for improvement in denoising performance of any given image. As a result, the bounds for natural images are usually much higher. The room for improvement for natural images can also be seen to be much lower than those for the synthetic images used in our study. Even for these natural images, the plots at low SNRs can be segregated into two regions.

From the above discussion, it becomes apparent that image denoising as a problem is not dead – yet. This is particularly true for the class of smoother images containing sufficiently large number of repeating patterns. On the surface, this may appear to be in direct contradiction to the observations in where Levin and Nadler compared the bounds to the best denoising methods and concluded that the performance of current non-parametric approaches cannot be improved upon, unless considerably larger patches are used.

IV. CONCLUSION AND FUTURE WORK

In this paper, we study image de-noising by using sliced ridgelets. It tries to remove the Gaussian white noise presented in the noisy images and also alleviates the limitations of wavelet and general ridgelet problems. Recent trends in ridgelet transforms proven that they are better than wavelet transforms to reduce the noise in images. This thesis concentrates on improvising the features of ridgelet transform to perform well than what it stands. As per our concern there is a wide research area and scope is still waiting for research concentration in ridigelet transforms.

This research work compares the accuracy and scalability of image de-noising with other popular approaches like wavelets, curvlets and some other inter-relevant technologies. We test our new denoising method with several standard images with Gaussian white noise added to the images. A very simple hard thresholding of the complex ridgelet coefficients is used. Experimental results show that complex ridgelets give better denoising results than VisuShrink, wiener2, and the ordinary ridgelets under all experiments. We suggest that ComRidgeletShrinkbe used for practical image donoising applications. Experimental results are proven that the sliced ridgelet approach is having the better performance than the other popular techniques.

Future work: Future work will be done by considering sliced ridgelets in curvelets image de-noising. Also, complexridgelets could be applied to extract invariant features for pattern recognition.

The computational cost of the sliced ridgelet transform is bit higher than that of ridgelets, especially in terms of 3D problems. We set the goal of reducing the computational cost of sliced ridgelets than general ridgelets is the another area of future research.

References

1. V.Krishna Naik, Prof.Dr.G.Manoj Someswar, R.B. Dayananda “Sliced Ridgelet Transform for Image De-noising” IOSR Journal of Computer Engineering (IOSR-JCE), e-ISSN: 2278-0661, p- ISSN: 2278-8727Volume 14, Issue 1 (Sep. - Oct. 2013), PP 17-21;
2. Jean-Luc Starck, Emmanuel J. Candès, and David L. Donoho “The Curvelet Transform for Image De-noising” IEEE TRANSACTIONS ON IMAGE PROCESSING, VOL. 11, NO. 6, JUNE 2002.
3. E. Cand’es, D. Donoho, Ridgelets: A key to higher-dimensional intermittency?, R. Soc. Lond. Philos. Trans. Ser. A Math. Phys. Eng. Sci., 357, 2495-2509 (1999).

4. B. Zhang, J. Fadili, J. Starck, Wavelets, ridgelets, and curvelets for Poisson noise removal, *IEEE Trans. Image Process.*, 17 (7), 10931108 (2008).
5. J. Ma, M. Fenn, Combined complex ridgelet shrinkage and total variation minimization, *SIAM J. Sci. Comput.*, 28 (3), 984-1000 (2006).
6. R. Coifman and D. Donoho. Wavelets and Statistics, chapter Translation invariant de-noising, pages 125–150. Springer-Verlag, 1995.
7. Hyeokho Choi and Richard G. Baraniuk. Multiple Wavelet Basis Image Denoising Using Besov Ball Projections. *IEEE Signal Processing Letters*, 11, no. 9: 717 – 720, 2004.
8. S. Barber and G. P. Nason. Real nonparametric regression using complex wavelets. *J. Roy. Stat. Soc. B*, 66, no. 4: 927 – 939, 2004.
9. H. Chauris, T. Nguyen, Seismic demigration/migration in the curvelet domain, *Geophysics*, 73 (2), S35-S46 (2008).
10. A. Antoniadis and J. Fan. Regularization of wavelet approximations. *Journal of the American Statistical Association*, 96, no. 455:939 – 955, 2001.
11. I. Adam, C. Naornita, J.-M. Boucher, and Al. Isar. A New Implementation of the Hyperanalytic Wavelet Transform. In *Proceedings of IEEE International Symposium ISSCS07, Iasi, Romania , 2007*.
12. Abdourrahmane M. Atto, Dominique Pastor, and Gregoire Mercier. Smooth Sigmoid Wavelet Shrinkage For Non-Parametric Estimation. In *IEEE International Conference on Acoustics, Speech and Signal Processing, ICASSP, Las Vegas, Nevada, USA, 30 march - 2008*.
13. E. Candès, L. Demanet, Curvelets and Fourier integral operators, *C. R. Math. Acad. Sci.Paris*, 336 (5), 395-398 (2003).
14. L. Demanet, L. Ying, Curvelets and wave atoms for mirror-extend images, *Proc. SPIE Wavelets XII, San Diego, August 2007*.
15. A. Cordoba, C. Fefferman, Wave packets and Fourier integral operators, *Comm. Partial Differential Equations*, 3, 979-1005 (1978).
16. GM.N. Do, M. Vetterli, The finite ridgelet transform for image representation, *IEEE Trans. Image Process.* 12 (1) (2003) 16–28.E.J.
17. Candes, Ridgelets: theory and applications, Ph.D. Thesis, Technical Report, Department of Statistics, Stanford University, 1998.